

Strong Final State Interactions in $\gamma\gamma \rightarrow WW$

P. Poulose¹ and L.M. Sehgal²

Institute for Theoretical Physics E
RWTH Aachen, D-52056 Aachen, Germany

Abstract

We study the effects of a possible strong final state interaction among longitudinal W 's in $\gamma\gamma \rightarrow WW$. The relevant partial wave amplitudes are modified by an Omnès function approximated by a Breit-Wigner form factor. We study the fractional cross section $f_{00} = \sigma_{LL}/\sigma_{\text{Total}}$ with both W 's longitudinally polarised, in the presence of a $J = 2$ resonance ($M = 2.5$ TeV, $\Gamma = 500$ GeV) or a $J = 0$ resonance ($M = 1$ TeV, $\Gamma = 1$ TeV), whose parameters are scaled up from the f_2 and σ resonances in the $\pi\pi$ system. We also examine the effects of final state interaction in the case of polarised photons ($J_z = 0$ or $J_z = 2$), and the impact on the Drell-Hearn-Gerasimov sum rule.

¹poulos@physik.rwth-aachen.de

²sehgal@physik.rwth-aachen.de

1 Introduction

The mechanism of electroweak symmetry breaking and the associated question of the origin of masses of particles is a central issue in our understanding of nature at a fundamental level. The Higgs mechanism employed in the standard model (SM) leads to the prediction of an elementary scalar particle with a mass $m_H = \sqrt{\lambda} v$, where $v = (\sqrt{2} G_F)^{-\frac{1}{2}} = 246$ GeV, and λ is the quartic coupling of the scalar potential. If the coupling λ is very large, however, the scalar sector becomes strongly interacting, and the above relation for the Higgs mass breaks down. In these circumstances, even the existence of an elementary scalar particle becomes questionable. Instead, the dynamics of the electroweak Goldstone bosons, which manifest themselves as the longitudinal components of the gauge fields W^\pm and Z , begins to resemble the dynamics of the π^\pm , π^0 mesons, which are the Goldstone bosons of chiral symmetry breaking in hadronic physics. In such a situation, it is reasonable to expect resonances in the strong interaction of longitudinal gauge bosons analogous to the σ , ρ , f_2 , etc., in the $\pi\pi$ system. The possibility of strong electroweak symmetry breaking is, therefore, best studied by analysing processes involving W_L 's and Z_L 's.

Such a situation has been considered in the literature in various reactions. A ρ -like resonance in the electroweak sector affects the process $e^+e^- \rightarrow W^+W^-$. Model independent analysis of this process has been carried out by several authors [1]. A specific model under the name of BESS has been developed to study such new vector resonances [2]. While $e^+e^- \rightarrow W^+W^-$ is sensitive to the existence of a ρ -like resonance, possible scalar and tensor resonances, which are the equivalents of σ and f_2 in the hadronic system, are conveniently studied in processes like $\gamma\gamma \rightarrow W^+W^-$, ZZ . Studies in this direction have been carried out in [3].

In our earlier study of $e^+e^- \rightarrow W^+W^-$, the strong final state interaction (FSI) of the longitudinal W 's was implemented with the help of the BESS model, in which a ρ -like vector triplet arises as a consequence of an additional $SU(2)$ gauge symmetry [4]. Such spin-1 resonances do not arise in $\gamma\gamma$ collisions. For our present investigation of $\gamma\gamma \rightarrow W^+W^-$, we take a model independent approach, exploring the consequences of $J = 0$ and $J = 2$ resonances in the WW system, which modify particular partial waves in the amplitude. These resonances are taken to be the equivalents of σ and f_2 resonance in the $\pi\pi$ system.

The plan of the paper is as follows. In Section 2, we recall the salient features of the process $\gamma\gamma \rightarrow W^+W^-$ in the SM. In Section 3 we describe how strong final state interaction effects are included. In Section 4 we discuss observables sensitive to such modifications. We give our conclusions in Section 5.

2 $\gamma\gamma \rightarrow W^+W^-$ in the Standard Model

The process $\gamma\gamma \rightarrow W^+W^-$ in the Standard Model has t -channel and u -channel contributions through the exchange of a W , and a contact interaction term. The helicity amplitudes are given in the literature [5], and we reproduce those in the Appendix.

Beam polarisation can be achieved in the photon linear colliders, where Compton back scattering of polarised laser and electron beams is used to produce high energy

photon beams [6]. The two independent polarisation combinations of the photon beams are those with same and opposite helicities. These are usually denoted by $J_z = \lambda_{\gamma_1} - \lambda_{\gamma_2} = 0$ and $J_z = 2$, where λ_{γ_1} and λ_{γ_2} are the helicities of the two photons. Differential cross sections corresponding to these two cases (summed over W polarisations) are given below.

$$\begin{aligned}\frac{d\sigma_{J_z=0}}{d\cos\theta} &= \frac{\beta}{8\pi s} \frac{(4\pi\alpha)^2}{(1-\beta^2\cos^2\theta)^2} (16 - 16r + 3r^2) \\ \frac{d\sigma_{J_z=2}}{d\cos\theta} &= \frac{\beta}{8\pi s} \frac{(4\pi\alpha)^2}{(1-\beta^2\cos^2\theta)^2} [(3 + 10r + 3r^2) + \\ &\quad 2(5 - 2r - 3r^2) \cos^2\theta + (3 - 6r + 3r^2) \cos^4\theta]\end{aligned}\tag{1}$$

Here, θ is the scattering angle, β is the velocity of W in the centre of mass frame, and $r = \frac{4m_w^2}{s}$. The unpolarised cross section is

$$\begin{aligned}\frac{d\sigma}{d\cos\theta} &= \frac{1}{2} \left(\frac{d\sigma_{J_z=0}}{d\cos\theta} + \frac{d\sigma_{J_z=2}}{d\cos\theta} \right) \\ &= \frac{\beta}{16\pi s} \frac{(4\pi\alpha)^2}{(1-\beta^2\cos^2\theta)^2} \{ (19 - 6r + 6r^2) + \\ &\quad 2(5 - 2r - 3r^2) \cos^2\theta + (3 - 6r + 3r^2) \cos^4\theta \}\end{aligned}\tag{2}$$

Both $J_z = 0$ and $J_z = 2$ distributions peak along the beam directions. Integrated cross sections in the case of polarised beams have the following expressions:

$$\begin{aligned}\sigma_{J_z=0}(s) &= \frac{\beta}{8\pi s} (4\pi\alpha)^2 \left\{ \left(\frac{16}{r} - 16 + 3r \right) + (16 - 16r + 3r^2) \frac{L}{2\beta} \right\} \\ \sigma_{J_z=2}(s) &= \frac{\beta}{8\pi s} (4\pi\alpha)^2 \left\{ \left(\frac{16}{r} + 22 + 3r \right) + (-16 + 4r + 3r^2) \frac{L}{2\beta} \right\}\end{aligned}\tag{3}$$

where $L = \log\left(\frac{1+\beta}{1-\beta}\right)$.

Notice that asymptotically these cross sections become equal, and the unpolarised cross section saturates to $\sigma(s \rightarrow \infty) = \frac{(4\pi\alpha)^2}{2\pi m_w^2} \sim 80.9$ pb. This advantage of $\gamma\gamma \rightarrow W^+W^-$ over other processes like $e^+e^- \rightarrow W^+W^-$, which decrease with s , makes it an attractive process in the linear colliders running at high energies.

The difference of the cross sections in Eq. 3

$$\Delta\sigma = \sigma_{J_z=2} - \sigma_{J_z=0} = \frac{\beta}{8\pi s} (4\pi\alpha)^2 \left\{ 38 + (-32 + 20r) \frac{L}{2\beta} \right\}\tag{4}$$

fulfills the sum rule

$$\int_{\frac{4m_W^2}{s}}^{\infty} \frac{\Delta\sigma(s)}{s} ds = 0. \quad (5)$$

This is a special case of the generalized Drell-Hearn-Gerasimov sum rule [7], which applies to any elementary process $\gamma + a \rightarrow b + c$ in a gauge theory, $\Delta\sigma$ being the cross section difference for parallel and antiparallel spins in the initial state. It is worth noting that $\Delta\sigma$ changes sign at $\sqrt{s} = 296$ GeV. Any new physics in the amplitude of $\gamma\gamma \rightarrow W^+W^-$ is likely to shift the location of this zero, and affect the convergence of the sum rule.

Finally we quote the $\gamma\gamma \rightarrow W^+W^-$ cross section for longitudinal W 's. The angular distributions and integrated cross section for the production of $W_L W_L$ are the following.

$$\begin{aligned} \frac{d\sigma_{J_z=0}^{W_L W_L}}{d\cos\theta} &= \frac{\beta}{8\pi s} \frac{(4\pi\alpha)^2}{(1 - \beta^2 \cos^2\theta)^2} r^2 \\ \frac{d\sigma_{J_z=2}^{W_L W_L}}{d\cos\theta} &= \frac{\beta}{8\pi s} \frac{(4\pi\alpha)^2}{(1 - \beta^2 \cos^2\theta)^2} (1 + r)^2 \sin^4\theta \end{aligned} \quad (6)$$

$$\begin{aligned} \sigma_{J_z=0}^{W_L W_L} &= \frac{\beta}{8\pi s} (4\pi\alpha)^2 \left[r + r^2 \frac{L}{2\beta} \right] \\ \sigma_{J_z=2}^{W_L W_L} &= \frac{\beta}{8\pi s} (4\pi\alpha)^2 \frac{(1 + r)^2}{\beta^2} \left[(2 + r) + r(r - 4) \frac{L}{2\beta} \right] \end{aligned} \quad (7)$$

Whereas the total cross section, summed over the WW polarisations, goes to a constant at high energy, the $W_L W_L$ fraction decreases with s . This fraction is of particular interest as a probe of FSI involving longitudinally polarised W 's.

In the following section we will discuss how the FSI is introduced by modifying particular partial waves, and how this affects various observables.

3 Strong Final State Interactions

As mentioned in the introduction, we assume the existence of strong interactions among longitudinal gauge bosons, analogous to the case of the $\pi\pi$ system. Final state interaction in the $\pi\pi$ system is known to introduce a phase shift in specific partial waves [8], which may be parametrised in terms of an Omnès function $\Omega(s)$ [9]. The partial wave amplitude in the presence of FSI is then modified according to

$$M^J \rightarrow \Omega^J(s) M^J \quad (8)$$

In the following we describe the partial wave decomposition of the amplitude of the process $\gamma\gamma \rightarrow W_L W_L$, and how the FSI is introduced. The relevant helicity amplitudes have the expansion [10]

$$M_{\lambda_{\gamma_1} \lambda_{\gamma_2} 00}^{SM}(s, \theta) = \sum_J \frac{(2J+1)}{4\pi} d_{J_z,0}^{J*}(\theta) M_{\lambda_{\gamma_1} \lambda_{\gamma_2} 00}^J(s) \quad (9)$$

Here $d_{J_z,0}^J(\theta)$ with $J_z = \lambda_{\gamma_1} - \lambda_{\gamma_2}$ are the rotation functions corresponding to the helicities considered.

Inverting Eq.9 using the orthogonality of the rotation functions, we get the partial wave amplitudes

$$M_{\lambda_{\gamma_1} \lambda_{\gamma_2} 00}^J(s) = (2\pi) \int d\cos\theta d_{J_z,0}^J(\theta) M_{\lambda_{\gamma_1} \lambda_{\gamma_2} 00}^{SM}(s, \theta) \quad (10)$$

As in the case of the $\pi\pi$ system [11], we expect the FSI to induce resonances of specific spins J_R . Such a resonance affects the partial wave amplitude $M_{\lambda_{\gamma_1} \lambda_{\gamma_2} 00}^{J_R}$. In the case of $\gamma\gamma$ collisions, only even values of J_R are allowed, and we will consider $J_R = 0$ and $J_R = 2$ resonances. In accordance with Eq. 8, we introduce these effects through an Omnès function $\Omega(s)$. For simplicity, we approximate this function by a Breit-Wigner function normalised to unity at the threshold. That is,

$$M_{\lambda_{\gamma_1} \lambda_{\gamma_2} 00}^{J_R}(s) \rightarrow \Omega^{J_R}(s) M_{\lambda_{\gamma_1} \lambda_{\gamma_2} 00}^{J_R}(s), \quad (11)$$

with

$$\Omega^{J_R}(s) = \frac{4m_w^2 - m_R^2}{s - m_R^2 + i \Gamma_R m_R \left(\frac{\beta}{\beta_R}\right)^{(2J_R+1)}} \quad (12)$$

Here, m_R is the mass and Γ_R the width of the resonance, $\beta = \sqrt{1 - 4m_w^2/s}$ and $\beta_R = \sqrt{1 - 4m_w^2/m_R^2}$. This modifies the helicity amplitudes such that

$$\begin{aligned} M_{\lambda_{\gamma_1} \lambda_{\gamma_2} 00}(s, \theta) &= \sum_J \frac{(2J+1)}{4\pi} d_{J_z,0}^{J*}(\theta) M_{\lambda_{\gamma_1} \lambda_{\gamma_2} 00}^J(s) \\ &= M_{\lambda_{\gamma_1} \lambda_{\gamma_2} 00}^{SM}(s, \theta) + [\Omega^{J_R}(s) - 1] \frac{2J_R + 1}{4\pi} d_{J_z,0}^{J_R*}(\theta) M_{\lambda_{\gamma_1} \lambda_{\gamma_2} 00}^{J_R}(s) \end{aligned} \quad (13)$$

where the superscript SM denotes the standard model result.

Expressions for the relevant $d_{J_z,0}^{J_R}$ functions and partial wave amplitudes are given in the Appendix. With the modified helicity amplitudes in Eq. 13, differential cross sections given in Eq. 1 are changed to

$$\begin{aligned}
\frac{d\sigma_{J_z=0}}{d\cos\theta} \Big|_{J_R=0} &= \frac{d\sigma_{J_z=0}^{SM}}{d\cos\theta} + \frac{\beta}{32\pi s} (4\pi\alpha)^2 \\
&\quad \times \left\{ 2 \operatorname{Re}(\Omega - 1) \frac{2r^2 L}{\beta (1 - \beta^2 \cos^2\theta)} + |\Omega - 1|^2 \frac{r^2 L^2}{\beta^2} \right\} \\
\frac{d\sigma_{J_z=0}}{d\cos\theta} \Big|_{J_R=2} &= \frac{d\sigma_{J_z=0}^{SM}}{d\cos\theta} + \frac{\beta}{32\pi s} (4\pi\alpha)^2 \\
&\quad \times \left\{ 2 \operatorname{Re}(\Omega - 1) \frac{5}{\beta^2} 2r^2 \left[-3 + (2+r) \frac{L}{2\beta} \right] \frac{3 \cos^2\theta - 1}{1 - \beta^2 \cos^2\theta} + \right. \\
&\quad \left. |\Omega - 1|^2 \left(\frac{5}{\beta^2} \right)^2 r^2 \left[-3 + (2+r) \frac{L}{2\beta} \right]^2 (3 \cos^2\theta - 1)^2 \right\} \\
\frac{d\sigma_{J_z=2}}{d\cos\theta} \Big|_{J_R=2} &= \frac{d\sigma_{J_z=2}^{SM}}{d\cos\theta} + \frac{\beta}{32\pi s} (4\pi\alpha)^2 \\
&\quad \times \left\{ 2 \operatorname{Re}(\Omega - 1) \frac{5}{2\beta^4} (1+r)^2 \left[(2-5r) + 3r^2 \frac{L}{2\beta} \right] \frac{\sin^4\theta}{1 - \beta^2 \cos^2\theta} + \right. \\
&\quad \left. |\Omega - 1|^2 \left(\frac{5}{4\beta^4} \right)^2 (1+r)^2 \left[(2-5r) + 3r^2 \frac{L}{2\beta} \right]^2 \sin^4\theta \right\}
\end{aligned} \tag{14}$$

For convenience we have dropped the labels on Ω . The expressions for Ω in the case of $J_R = 0$ and $J_R = 2$ differ according to Eq. 12. Corresponding integrated cross sections are given by

$$\begin{aligned}
\sigma_{J_z=0}(s) \Big|_{J_R=0} &= \sigma_{J_z=0}^{SM}(s) + (2 \operatorname{Re}(\Omega - 1) + |\Omega - 1|^2) \frac{(4\pi\alpha)^2}{16\pi s} \frac{r^2}{\beta} L^2 \\
\sigma_{J_z=0}(s) \Big|_{J_R=2} &= \sigma_{J_z=0}^{SM}(s) + (2 \operatorname{Re}(\Omega - 1) + |\Omega - 1|^2) \\
&\quad \times \frac{(4\pi\alpha)^2}{16\pi s} \frac{5r^2}{\beta^3} \left[-3 + (2+r) \frac{L}{2\beta} \right]^2 \\
\sigma_{J_z=2}(s) \Big|_{J_R=2} &= \sigma_{J_z=2}^{SM}(s) + (2 \operatorname{Re}(\Omega - 1) + |\Omega - 1|^2) \\
&\quad \times \frac{(4\pi\alpha)^2}{16\pi s} \frac{5}{6} \frac{(1+r)^2}{\beta^7} \left[(2-5r) + 3r^2 \frac{L}{2\beta} \right]^2
\end{aligned} \tag{15}$$

The above equations are used to analyse how various cross sections are modified. We discuss the numerical results in the next section.

4 Numerical Results

In our numerical analysis we have considered spin-0 and spin-2 resonances analogous to σ and f_2 in the $\pi\pi$ system, scaled up to $m_R = 1$ TeV and $\Gamma_R = 1$ TeV; and $m_R = 2.5$ TeV and $\Gamma_R = 0.5$ GeV respectively, using a rough scaling factor of $v/f_\pi \sim 2000$, where f_π is the π decay constant. We keep in mind a photon-collider operating at and above 500 GeV centre of mass energy, as is expected, for example in TESLA. We also consider the polarisation option, which is expected to be achieved in photon-linear colliders. Our principal results are as follows.

1. Fig. 1a shows cross sections versus \sqrt{s} separately for the polarisation states $J_z = 0$ and $J_z = 2$. The effects of the resonances are essentially invisible on this scale. To increase the sensitivity to FSI, we consider the cross section with an angular cut $|\cos\theta| \leq 0.8$. This, for the case of $J_R = 2$ is shown in Fig. 1b, where the resonant enhancement is visible. For the $J_R = 0$ resonance, the enhancement is essentially invisible even after the angular cut.

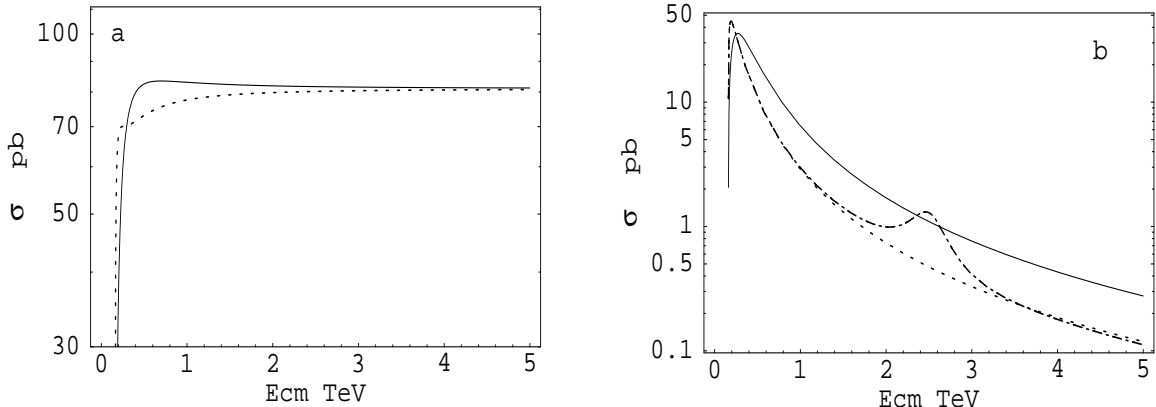


Figure 1: Cross section of unpolarised W 's (a) without any cut, and (b) with an angular cut of $|\cos\theta| \leq 0.8$. Solid and dotted curves correspond to $J_z = 2$ and $J_z = 0$ respectively, in the SM. The dash-dotted curve in (b) shows the effect of a $J_R = 2$ final state resonance.

2. In Fig. 2a we show a plot of σ_{LL} (the cross section for $W_L W_L$) versus \sqrt{s} , with and without the $J = 0$ and $J = 2$ resonances. The effects of an angular cut are indicated in Fig. 2b. Clearly, the effects of final state interaction become more visible when the longitudinal part of the cross section (σ_{LL}) is isolated.

3. The longitudinal fraction of the cross section, defined as

$$f_{00} = \frac{\sigma_{LL}}{\sigma_{\text{tot}}},$$

is given in Table 1. Values of f_{00} are listed in the SM and in the presence of FSI with and without an angular cut. One can observe that, with an angular cut $|\cos\theta| \leq 0.8$, the fraction f_{00} increases typically from 3% in the SM to 4% in the presence of FSI. It may be recalled that the parameter f_{00} can be determined empirically by studying the energy distribution of the secondary leptons from the W 's (see Ref.[12]).

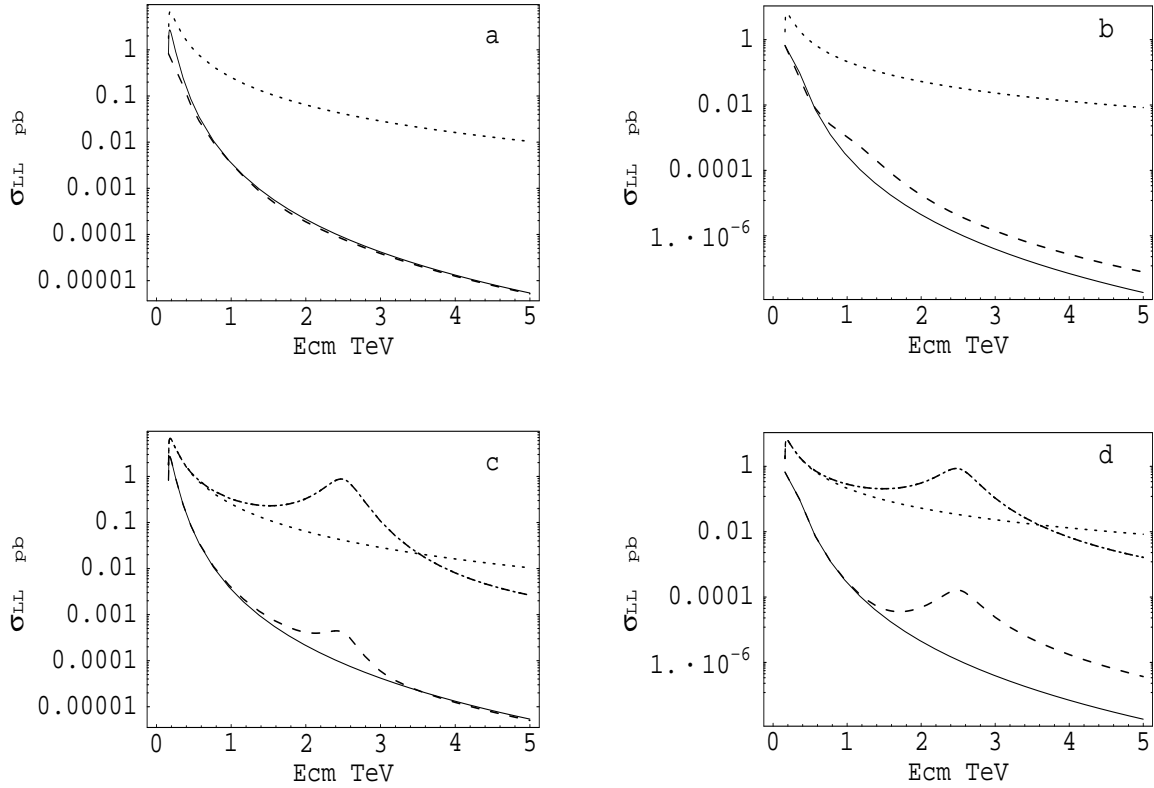


Figure 2: Cross section for longitudinally polarised W 's. (a) and (c) are without angular cut, while (b) and (d) are for $|\cos \theta| \leq 0.8$. Effects of $J_R = 0$ are shown in (a) and (b), and for $J_R = 2$ in (c) and (d). Solid and dotted lines correspond to the SM results for $J_z = 0$ and $J_z = 2$ respectively, while the dashed and dash-dotted curves include FSI.

4. Finally, we show in Fig. 3 the cross section difference $\Delta\sigma = \sigma_{J_z=2} - \sigma_{J_z=0}$ as a function of \sqrt{s} . The zero of the function, which in the SM lies at $\sqrt{s} = 296$ GeV, is shifted upwards by about 1 GeV. The integral (Eq. 5) is no longer convergent, as is to be expected when gauge theory amplitudes are modified by an unconventional WW interaction introduced in a phenomenological way.

5 Conclusions

We have investigated the effects of strong $W_L^+W_L^-$ interaction in the channel $\gamma\gamma \rightarrow W^+W^-$, assuming resonant structures analogous to the σ and f_2 resonances in the $\pi\pi$ system. Numerical corrections to the standard model predictions have been evaluated for the total cross section, and for the longitudinal fraction, $f_{00} = \sigma_{LL}/\sigma_{\text{tot}}$. A typical result is an enhancement of f_{00} from 3% to about 4% at $\sqrt{s} = 500$ GeV, after inclusion of an angular cut $|\cos \theta| \leq 0.8$. We have also calculated the cross section difference, $\Delta\sigma = \sigma_{J_z=2} - \sigma_{J_z=0}$ for like and unlike photon polarisations in the initial state, which

		No angular cut			$ \cos \theta \leq 0.8$		
		500	800	1000	500	800	1000
σ^{SM} (pb)		77.82	79.90	80.32	15.75	7.05	4.66
f_{00}	SM	0.0068	0.0025	0.0016	0.029	0.024	0.023
	$SM+FSI(J_R = 0)$	0.0122	0.0036	0.0021	0.045	0.030	0.027
	$SM+FSI(J_R = 2)$	0.0125	0.0040	0.0026	0.046	0.034	0.034

Table 1: Longitudinal fraction of cross section, $f_{00} = \sigma_{LL}/\sigma_{\text{tot}}$ with and without angular cut. Values of f_{00} in the presence of FSI with $J_R = 0$ and $J_R = 2$ resonances are shown along with the SM values, for different centre of mass energies of the collider.

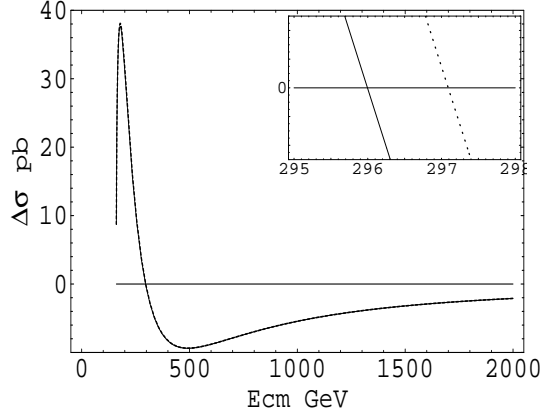


Figure 3: $\Delta\sigma$ against \sqrt{s} . Inset shows the shift in the position of zero (dotted line) in the presence of strong FSI with $J_R = 0$ resonance at $m_R = 1$ TeV and $\Gamma_R = 1$ TeV.

is relevant to the generalized DHG sum rule. The zero of $\Delta\sigma(s)$, which occurs at 296 GeV in the SM, is shifted upwards by about 1 GeV in the presence of FSI.

Acknowledgements

One of us, P.P. wishes to thank the Humboldt Foundation for a Post-doctoral Fellowship, and the Institute of Theoretical Physics E, RWTH Aachen for the hospitality provided during this work.

Appendix A: Helicity Amplitudes

Following are the helicity amplitudes of the process $\gamma\gamma \rightarrow W^+W^-$ in the Standard

Model, norlamised such that,

$$\frac{d\sigma}{d \cos \theta} = \frac{\beta}{32\pi s} \sum_{\lambda} |M_{(\lambda_{\gamma_1}, \lambda_{\gamma_2}, \lambda_{w^-}, \lambda_{w^+})}^{SM}(s, \cos \theta)|^2 \quad (16)$$

with $\lambda_{\gamma_1}, \lambda_{\gamma_2}, \lambda_{w^-}$ and λ_{w^+} are helicities of initial photon beams and W 's produced; \sqrt{s} , the centre of mass energy; θ the scattering angle in the c.m.f. Summation over final particle helicities, and averaging over initial state helicites are implied by \sum_{λ} .

Taking out a common factor, the helicity amplitudes are expressed in terms of the functions $A_{(\lambda_{\gamma_1}, \lambda_{\gamma_2}, \lambda_{w^-}, \lambda_{w^+})}$ as

$$M_{(\lambda_{\gamma_1}, \lambda_{\gamma_2}, \lambda_{w^-}, \lambda_{w^+})}^{SM}(s, \cos \theta) = \frac{4\pi\alpha}{1 - \beta^2 \cos^2 \theta} A_{(\lambda_{\gamma_1}, \lambda_{\gamma_2}, \lambda_{w^-}, \lambda_{w^+})}^{SM}(s, \cos \theta), \quad (17)$$

with

$$\begin{aligned} A_{\pm\pm 00}^{SM} &= 2r \\ A_{\pm\pm\pm\pm}^{SM} &= 2(1+\beta)^2 \\ A_{\pm\pm\mp\mp}^{SM} &= 2(1-\beta)^2 \\ A_{\pm\mp 00}^{SM} &= -2(1+r)\sin^2\theta \\ A_{\pm\mp 0\pm}^{SM} &= \mp 2\sqrt{2r}(1-\cos\theta)\sin\theta = A_{\mp\pm\pm 0}^{SM} \\ A_{\pm\mp 0\mp}^{SM} &= \mp 2\sqrt{2r}(1+\cos\theta)\sin\theta = A_{\mp\pm\mp 0}^{SM} \\ A_{\pm\mp\pm\pm}^{SM} &= 2r\sin^2\theta = A_{\mp\pm\pm\pm}^{SM} \\ A_{\pm\mp\pm\mp}^{SM} &= 2(1+\cos\theta)^2 \\ A_{\pm\mp\mp\pm}^{SM} &= 2(1-\cos\theta)^2 \end{aligned} \quad (18)$$

where $r = \frac{4m_w^2}{s}$. All other helicity amplitudes vanish.

Appendix B: Partial Wave Amplitudes

Partial wave amplitudes are given in terms of the helicity amplitudes as,

$$M_{\lambda_{\gamma_1}, \lambda_{\gamma_2}, \lambda_{w^-}, \lambda_{w^+}}^J(s) = (2\pi) \int d \cos \theta d_{\delta_{\gamma}, \delta_w}^J(\theta) M_{\lambda_{\gamma_1}, \lambda_{\gamma_2}, \lambda_{w^-}, \lambda_{w^+}}^{SM}(s, \theta) \quad (19)$$

Here $\delta_{\gamma} = \lambda_{\gamma_1} - \lambda_{\gamma_2}$ and $\delta_w = \lambda_{w^-} - \lambda_{w^+}$. Partial wave amplitudes that are relevant in the present case are the following:

$$M_{\pm\pm 00}^{J_R=0}(s) = 4\pi\alpha \frac{4\pi r}{\beta} \log\left(\frac{1+\beta}{1-\beta}\right)$$

$$\begin{aligned}
M_{\pm\mp 00}^{J_R=2}(s) &= 4\pi\alpha \frac{4\pi r}{\beta^2} \left[-3 + \frac{2+r}{2\beta} \log\left(\frac{1+\beta}{1-\beta}\right) \right] \\
M_{\pm\mp 00}^{J_R=2}(s) &= -4\pi\alpha \frac{4\pi (1+r)}{\sqrt{6} \beta^4} \left[(2-5r) + \frac{3r^2}{2\beta} \log\left(\frac{1+\beta}{1-\beta}\right) \right]
\end{aligned} \tag{20}$$

We have used the following d functions:

$$\begin{aligned}
d_{0,0}^0 &= 1 \\
d_{0,0}^2 &= \frac{1}{2} (3 \cos^2 \theta - 1) \\
d_{2,0}^2 &= \sqrt{\frac{3}{8}} \sin^2 \theta = d_{-2,0}^2
\end{aligned} \tag{21}$$

References

- [1] T.L.Barklow, *hep-ph/0112286* and references therein; see also: T.L.Barklow, R.S.Chivukula, J. Goldstein, T. Han, *hep-ph/0201243*; R.D. Heuer, D. Miller, F. Richard, P. Zerwas, *TESLA Technical Design Report: Part III, DESY-2001-011 (hep-ph/0106315)*; T.L.Barklow,G.Burdman,R.S.Chivukula, B.A. Dobrescu, P.S. Drell,N.Hadley, W.B. Kilgore, M. E. Peskin,J.Terning ,D.R. Wood, *hep-ph/9704217*;
- [2] R. Casalbuoni, S. De Curtis, D. Dominici, R. Gatto, *Phys. Lett. B* **155** (1985) 95; *Nucl. Phys. B* **282** (1987) 235;
- [3] E.E. Boos and G.V.Jikia, *Phys. Lett. B* **275** (1992) 164; M. Herrero and E. Ruiz-Morales, *Phys. Lett. B* **296** (1992) 397; A. Abbasabadi, David Bowser-Chao, Duane A. Dicus, Wayne W. Repko, *Phys. Rev. D* **4** (1994) 547; M.S. Berger, Michael S. Chanowitz, *Nucl. Inst. Meth. A* **355** (1995) 52.
- [4] P. Poulose, S.D. Rindani, L.M. Sehgal, *Phys. Lett. B* **525** (2002) 71
- [5] E. Yehudai, *Phys. Rev. D* **44** (1991) 3434; M. Baillargeon, G. Belanger, F. Boudjema , *Nucl. Phys. B* **500** (1997) 224.
- [6] I.F.Ginzburg, G.L. Kotkin, V.G. Serbo, V.I. Telnov, *Nucl. Inst. Meth. A* **205** (1983) 47; I.F.Ginzburg, G.L. Kotkin, S.L. Panfil, V.G. Serbo, V.I. Telnov, *Nucl. Inst. Meth. A* **219** (1984) 5; V. Telnov, *Nucl. Inst. Meth. A* **355** (1995) 3.
- [7] S.D.Drell and A.C.Hearn, *Phys. Rev. Lett.* **16** (1966) 908; S.B.Gerasimov, Sov. J. Nucl. Phys. **2** (1966) 430; G. Altarelli, N. Cabibbo, L. Maiani, *Phys. Lett. B* **40** (1972) 415; S. J. Brodsky, T. G. Rizzo and I. Schmidt, *Phys. Rev. D* **52** (1995) 4929
- [8] K. M. Watson, *Phys. Rev. 88* (1952) 1163

- [9] R. Omnès, Nuovo Cim. **8** (1958) 316
- [10] See, for example, A.D. Martin and T.D. Spearman, “*Elementary Particle Theory*” (1970), North-Holland Publishing Company.
- [11] D. Morgan, M.R. Pennington, Z. Phys. **C 37** (1988) 431, Erratum-*ibid.* **C 39** (1988) 590.
- [12] Anja Werthenbach, L.M. Sehgal, Phys. Lett. **B402** (1997) 189